



HAL
open science

Depletion interactions and fluid-solid equilibrium in emulsions

Jérôme Bibette, Didier Roux, Frédéric Nallet

► **To cite this version:**

Jérôme Bibette, Didier Roux, Frédéric Nallet. Depletion interactions and fluid-solid equilibrium in emulsions. *Physical Review Letters*, 1990, 65 (19), pp.2470-2473. 10.1103/PhysRevLett.65.2470 . hal-04186464v2

HAL Id: hal-04186464

<https://hal.science/hal-04186464v2>

Submitted on 28 Aug 2023

HAL is a multi-disciplinary open access archive for the deposit and dissemination of scientific research documents, whether they are published or not. The documents may come from teaching and research institutions in France or abroad, or from public or private research centers.

L'archive ouverte pluridisciplinaire **HAL**, est destinée au dépôt et à la diffusion de documents scientifiques de niveau recherche, publiés ou non, émanant des établissements d'enseignement et de recherche français ou étrangers, des laboratoires publics ou privés.



Distributed under a Creative Commons Attribution 4.0 International License

Depletion Interactions and Fluid-Solid Equilibrium in Emulsions

J. Bibette, D. Roux, and F. Nallet

Centre de Recherche Paul-Pascal, Domaine Universitaire, F-33405 Talence CEDEX, France

(Received 12 April 1990)

Silicon-oil-in-water emulsions, stabilized with sodium dodecylsulfate (SDS), have been studied. They exhibit practically no coalescence, whereas for high surfactant concentrations a "creaming" of the emulsion is observed. We demonstrate that this behavior is related to a fluid-solid phase transition due to an attractive interaction induced by the depletion of SDS micelles. A simple model for the fluid-solid transition is proposed, in quantitative agreement with experiment.

PACS numbers: 82.70.Kj, 05.70.Fh, 64.70.Hz

Emulsions are metastable oil and water mixtures stabilized with a surfactant. Both oil-in-water and water-in-oil systems exist. They are extremely important for industrial applications such as cosmetology, the food industry, and oil recovery.¹ The structure can be described as droplets dispersed in a continuous phase. Most often, they are highly polydisperse systems: The size and polydispersity are strong functions of both the preparation scheme and time. The description of such systems is complex owing to the interplay between thermodynamics and kinetics. Indeed, on one hand emulsions can be described as classical colloidal suspensions (interacting spheres) and on the other hand they involve the time-dependent macroscopic separation of oil and water (coalescence). Nevertheless, in certain interesting cases (relevant for industrial applications), the characteristic coalescence time is extremely large.

As an example of a kinetically stable system, we have studied a silicon oil (polydimethylsiloxane) in water emulsion, stabilized with sodium dodecylsulfate (SDS).² The oil droplets exhibit practically no coalescence and there is no macroscopic oil-water separation for years. However, depending on the total surfactant concentration, our system displays a creaming effect, which takes place within a few hours. This effect is frequently encountered in various emulsions;³ it corresponds here to the reversible separation between a droplet-rich phase and a dilute one. In what follows, we demonstrate, using specially prepared monodisperse emulsions, that the creaming effect comes from a fluid-solid phase transition induced by attractive depletion forces, originating in the presence of SDS micelles. We show that emulsions, which are one of the most important industrial colloidal systems, can be used to do fundamental physics. Using light scattering, we were able to measure depletion interactions induced by the surfactant and to quantitatively compare them with theoretical predictions. With such emulsions, we present the first completely characterized liquid-solid equilibrium induced by attractive forces: phase-diagram analysis, measurements of interactions, and characterization of the structure of the solid using a phase-contrast microscope and Bragg scattering. This was made possible using an original method (fractionated crystallization) to get monodisperse droplets from a very polydisperse classical emulsion.

We have first studied the creaming effect on a typical polydisperse emulsion (oil volume fraction $\phi = 10\%$, droplet sizes between 0.2 and 5 μm) upon SDS concentration changes. Above roughly 0.05 mol l^{-1} of SDS, a dense phase made of aggregated oil droplets separates from a dilute phase of free droplets. A careful observation indicates that at the flocculation threshold the dense phase contains most of the bigger droplets, whereas the dilute one is made mainly of the smaller ones. This allowed us to prepare monodisperse emulsions of well-controlled diameters σ ($\Delta\sigma/\sigma = 10\%$), following a fractionated crystallization scheme.⁴ Phase diagrams in the surfactant concentration-oil volume fraction plane have been determined for monodisperse emulsions by observation under a microscope. They are shown in Fig. 1 for three different emulsion sizes (diameters σ of 0.93, 0.60, and 0.46 μm). The surfactant concentration is expressed as the volume fraction of SDS micelles [critical micellar concentration (CMC) is $8 \times 10^{-3} \text{ mol l}^{-1}$, micellar diameter $\sigma_0 = 40 \text{ \AA}$, and aggregation number of SDS micelles is 80]. The experimental points separate the one-phase region where only free droplets are observed (fluid

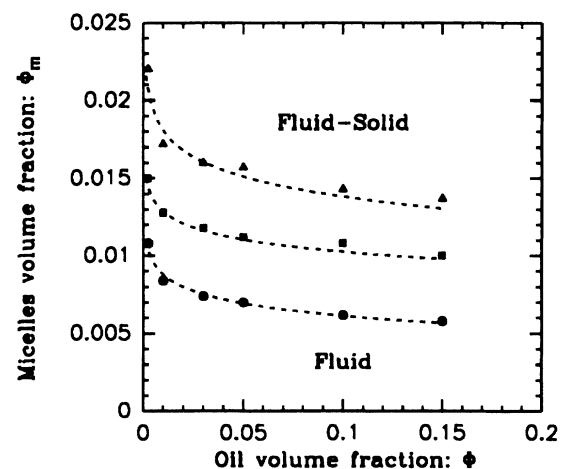


FIG. 1. Phase diagram in the micelle volume fraction vs oil-droplet volume fraction (ϕ_m, ϕ) plane. The droplet sizes are, respectively, 0.93 μm (circles), 0.60 μm (squares), and 0.46 μm (triangles). The dotted lines are theoretical predictions for the phase boundaries (see text below) and separate the one-phase region from the two-phase one.

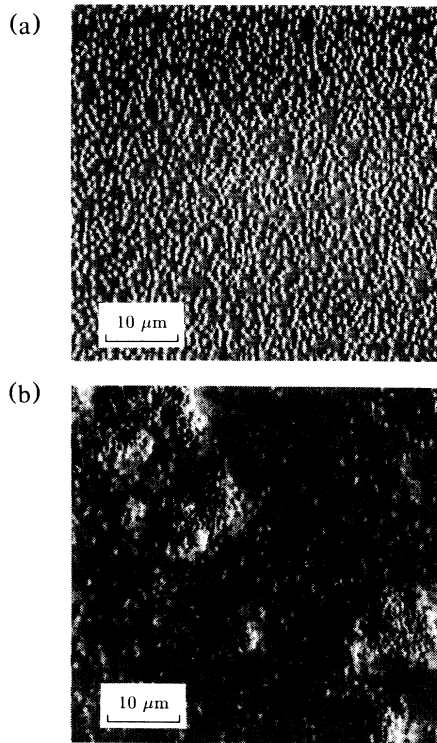


FIG. 2. Pictures taken in (a) the one-phase region and (b) the two-phase region, for a monodisperse emulsion characterized by oil-droplet diameter $\sigma \approx 0.7 \mu\text{m}$, oil volume fraction $\phi = 10\%$, and surfactant micelle volume fractions (a) $\phi_m = 0$ and (b) $\phi_m = 9.2 \times 10^{-3}$.

phase) from the two-phase region where aggregated and free droplets coexist. Note that the phase boundary is located at higher surfactant concentrations for smaller oil droplets. Moreover, a dynamic observation shows that, in addition to the Brownian motion, there is a continuous exchange of droplets between the dense and dilute phases: This hints at a thermodynamic equilibrium between the coexisting phases. Pictures taken in the one-phase (fluid) and the two-phase regions are present-

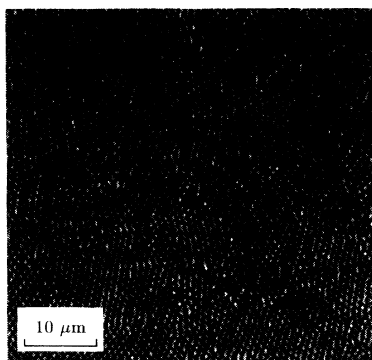


FIG. 3. A picture showing, on a polycrystalline sample, the long-range ordering of the dense phase. The droplet diameter is $\sigma = 0.93 \mu\text{m}$.

ed in Figs. 2(a) and 2(b), respectively.

Macroscopic samples of the dense phase are obtained after decantation. Figure 3 shows such a sample ($\sigma = 0.93 \mu\text{m}$) constrained between two glass plates $3 \mu\text{m}$ apart. The structure of a solid, with a long-range ordering of the oil droplets, is clearly observed. The crystalline structure of bulk samples (cell thickness 10 to $40 \mu\text{m}$) is demonstrated by light diffraction experiments with an argon-ion laser ($\lambda = 4880 \text{ \AA}$). For each sample studied, two Bragg reflections are recorded, as shown in Fig. 4(a) for one particular sample. The positions of the Bragg peaks are consistent with the fcc structure ($q_2/q_1 = 1.63 \pm 0.02$). Note that the same structure was observed in hard-sphere-like colloidal crystals.⁵ The droplet diameters σ are accurately deduced from the peak positions q_1 by the formula $\sigma = (\frac{3}{2})^{1/2} 2\pi/q_1$, with the assumption that close contact of the oil droplets fixes

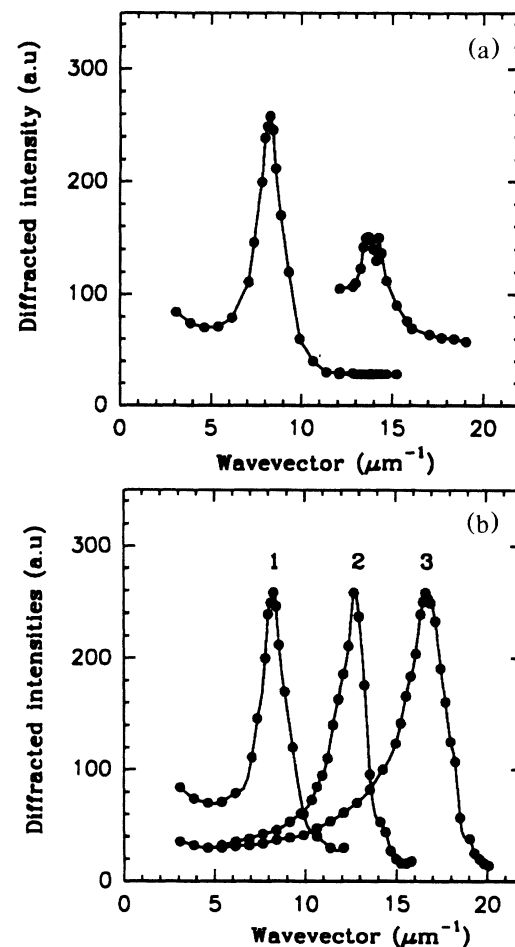


FIG. 4. (a) Diffracted intensities vs wave vector in the solid phase. Two diffraction peaks are found for each sample, which are compatible with a fcc structure (to make the second peak visible the intensity scale has been enhanced by a factor of 8). (b) The position of the first peak allows the precise measurement of the oil-droplet sizes: $\sigma = 0.93 \mu\text{m}$ (curve 1), $0.60 \mu\text{m}$ (curve 2), and $0.46 \mu\text{m}$ (curve 3).

the lattice parameter d_{111} . The relevant diffraction curves are reported in Fig. 4(b).

In order to explain consistently the phase diagram, attractive interactions must be evoked. A plausible attractive mechanism is a depletion interaction:³ When two oil droplets come too close to each other, the interdroplet spacing becomes an excluded volume for the micelles formed by the excess surfactant. The general mechanism for depletion interactions has been theoretically investigated and various effective short-range attractive potentials have been proposed.⁶⁻⁸ The ideal-gas approach developed by Vrij⁷ is appropriate to the description of the depletion of dilute, small spherical objects, relevant to our study. The interaction range is found to be equal to the small-object diameter σ_0 ; the contact potential, in the limit of a large size asymmetry, is $\frac{3}{2}kT\sigma/\sigma_0\phi_m$, where ϕ_m is the volume fraction of the small objects. Up to now, some experimental evidence for a depletion interaction comes from studies of colloidal particles dispersed in nonadsorbing polymer solutions.⁹⁻¹¹

To demonstrate the micelle depletion mechanism, a light-scattering experiment has been performed on the fluid phase. The small objects responsible for the attractive interaction (SDS micelles; diameter $\sigma_0=40$ Å) have a negligible scattering compared to the one arising from the much bigger colloidal objects (oil droplets; σ about 1 μm). Besides, in spite of sizes comparable to the light wavelength, the oil-droplet scattering has been checked to follow the Rayleigh-Gans regime in the experimental wave-vector range. Therefore, the droplet-droplet structure factor is, in principle, easily recovered from the light-scattering spectra. Nevertheless, the samples are intrinsically very milky: Care should be taken to avoid multiple scattering. Very thin cells (20 μm) have been used, and we checked that no difference arises in the

scattering curves for thicknesses between 10 and 40 μm ; the transmission is always larger than 80%. Typical scattering data $I(q)$ as a function of the wave vector q [$q=4\pi n/\lambda \sin(\theta/2)$, with n the refractive index, λ the wavelength of the light, and θ the scattering angle] are shown in Fig. 5. The two curves correspond to the same droplet volume fraction ϕ ($\phi=0.17$), the samples differing only in their surfactant concentration ($\phi_m=0.012$, curve *a*; $\phi_m=0$, curve *b*). At low surfactant concentration a correlation peak dominates, indicating hard-sphere-like interactions, whereas at higher surfactant concentration, a strong small-angle scattering appears, indicating attractive interactions.

A quantitative study of the interactions is possible, fitting theoretical structure factors to the experimental curves. Since the wave-vector range is practically limited, the structure factor is not sensitive to the detailed nature of the potential: For simplicity, we choose to describe the attractive interactions by a square-well potential. The structure factor is then obtained using the mean-spherical-approximation scheme proposed by Sharma and Sharma¹² and improved by Huang *et al.*¹³ The square-well potential is characterized by three parameters: the hard-core diameter, which is taken to be σ , the measured oil droplet diameter; the range of the square well, σ_0 , the micellar diameter; and the depth, ε , which is the only free parameter in our study. The fitted depth of the potential, in kT units, as a function of the micelle volume fraction ϕ_m is shown in Fig. 6, for an emulsion with $\sigma=0.60$ μm at an oil volume fraction $\phi=0.17$. When no surfactant micelles are present, i.e., below CMC, there is a weak van der Waals background attraction. Above CMC, the attraction increases linearly with ϕ_m . This behavior confirms qualitatively the depletion mechanism. The straight line in Fig. 6 has a slope of 320. This compares quantitatively well with the

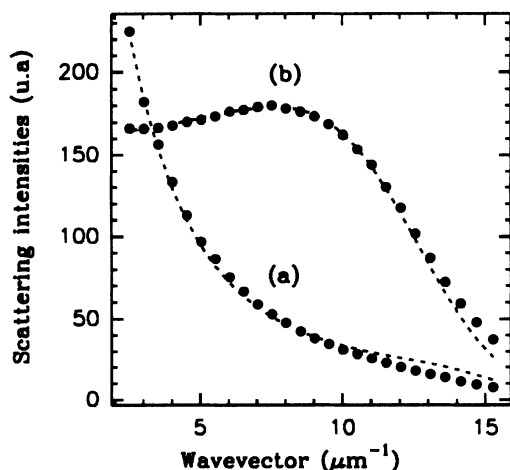


FIG. 5. Scattered intensities vs wave vector in the fluid phase of the $\sigma=0.46$ μm , $\phi=0.17$ emulsion, for two surfactant concentrations: $\phi_m=0.012$ (curve *a*) and $\phi_m=0$ (curve *b*). The dotted lines are theoretical predictions.

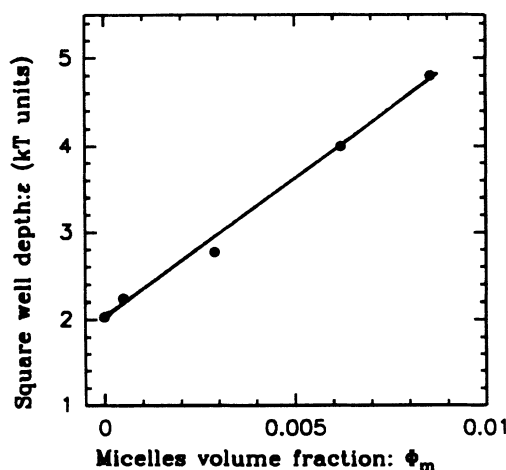


FIG. 6. Fitted square-well depth ε , in kT units, vs the micelle volume fraction ϕ_m . The linear behavior is consistent with the depletion model. The extrapolation at $\phi_m=0$ corresponds to an attractive background due to van der Waals attraction.

predicted slope $\frac{3}{2} \sigma/\sigma_0$, which is 225. The same agreement between fitted interactions and predictions from the depletion theory is observed when varying the droplet diameters.

Let us consider now the fluid-solid transition. Taking into account that the fluid phase is fairly dilute ($\phi < 20\%$) and the solid phase mostly incompressible and compact (oil volume fraction fixed at the close-contact value $\phi_s = 74\%$), we have worked out the following model. The fluid free-energy density is taken to be the ideal-gas one:

$$f_g = (kT/v)[\phi \ln \phi + \phi(\mu_g^0 - 1)],$$

where v is the volume of an oil droplet, and μ_g^0 the reference chemical potential. The solid free-energy density is derived from the Einstein model:

$$f_s = (kT/v)\phi_s(U_0 + \mu_s^0),$$

with μ_s^0 the reference chemical potential of the Einstein solid and U_0 the lattice contact potential [$U_0 = -\frac{1}{2}z(\frac{3}{2}\sigma/\sigma_0\phi_m + w)$; z is the nearest-neighbor number], taking into account both depletion (ϕ_m term) and van der Waals (w term) interactions. The oil volume fraction ϕ in the fluid phase at the coexistence point is the solution of the equation¹⁴

$$f_g + (\phi_s - \phi)df_g/d\phi = f_s.$$

With the expressions given above for f_g and f_s , we get (neglecting the linear term)

$$\phi_m = (\sigma_0/9\sigma)(-\ln\phi + \mu_s^0 - \mu_g^0 - w),$$

which is the equation of the phase boundary in the (ϕ, ϕ_m) plane. This is a two-parameter description of the phase diagram of the form $\phi_m = A(-\ln\phi + B)$. The parameters A and B are then extracted from a fit to the experimental phase diagram (see Fig. 1). From the parameter A we get a value for the ratio σ/σ_0 which is within 20% of the experimental value, whatever the sample studied. The parameter B , which encompasses the poorly known reference solid chemical potential, is in the range $(3-6)kT$.

We want to stress that these results could have been obtained with monodisperse droplets only. The purification method is based on the extreme sensibility of the liquid-solid transition (via the depletion interaction) to the droplet size: Monodisperse samples are obtained after a few crystallizations separating big particles (in

the crystal) from smaller ones (in the liquid).

We have demonstrated that the creaming phenomenon observed in noncoalescent oil-in-water emulsion is a liquid-solid phase transition that originates in an attractive depletion interaction. Surfactant micelles, always present in the emulsion, are responsible for this interaction. Using both light-scattering and phase-diagram analysis, we have proven the validity of the Vrij approach to depletion. The logarithmic shape of the phase boundary is a universal feature of a liquid-solid transition encountered in complex fluids of big colloidal objects.

The authors thank P. Bothorel, P. Peignier, and G. Schorsch for introducing them to emulsion science. They are very grateful to B. Pouligny and C. Coulon for fruitful discussions on many aspects of light scattering and statistical mechanics. They would like to thank P. Attard and L. Belloni. This work has been supported in part by Rhône-Poulenc Company.

¹K. J. Lissant, *Emulsion and Emulsion Technology* (Marcel Dekker, New York, 1974), Vol. 6.

²The polydisperse initial emulsion was provided by Rhône-Poulenc Co., Saint-Fons, France.

³M. P. Aronson, *Langmuir* **5**, 494 (1989).

⁴J. Bibette, French Patent No. 90/01990 (14.02.1990).

⁵P. N. Pusey, W. Van Meegen, P. Bartlett, B. J. Ackerson, J. G. Rarity, and S. M. Underwood, *Phys. Rev. Lett.* **63**, 2753 (1989).

⁶S. Asakura and F. Oosawa, *J. Chem. Phys.* **22**, 1255 (1954).

⁷A. Vrij, *Pure Appl. Chem.* **48**, 471 (1976).

⁸J.-F. Joanny, L. Leibler, and P.-G. De Gennes, *J. Polymer Sci. Polymer Phys. Ed.* **17**, 1073 (1979).

⁹P. R. Sperry, *J. Colloid Interface Sci.* **99**, 97 (1984).

¹⁰H. de Hek and A. Vrij, *J. Colloid Interface Sci.* **88**, 258 (1982).

¹¹A. P. Gast, W. B. Russel, and C. K. Hall, *J. Colloid Interface Sci.* **109**, 160 (1986).

¹²R. V. Sharma and K. C. Sharma, *Physica (Amsterdam)* **89A**, 213 (1977).

¹³J. S. Huang, S. A. Safran, M. W. Kim, G. S. Grest, M. Kotlarchyk, and M. Quirke, *Phys. Rev. Lett.* **53**, 592 (1984).

¹⁴The formula given in the text holds when the free energy in one phase has a very deep minimum; see e.g., D. Andelman, M. E. Cates, D. Roux, and S. A. Safran, *J. Chem. Phys.* **87**, 7229 (1987).

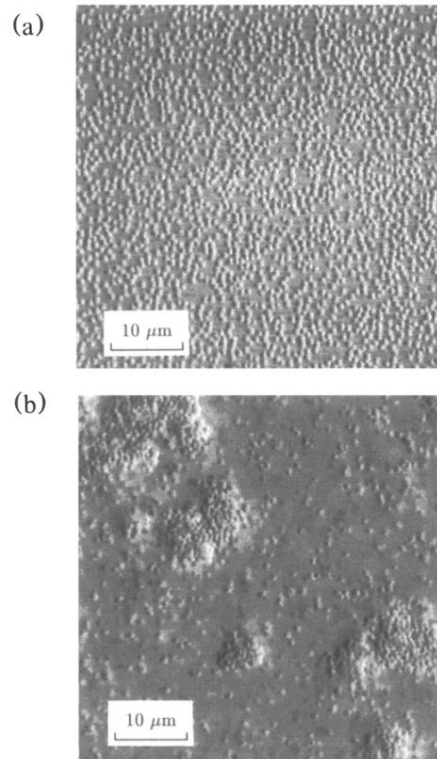


FIG. 2. Pictures taken in (a) the one-phase region and (b) the two-phase region, for a monodisperse emulsion characterized by oil-droplet diameter $\sigma \approx 0.7 \mu\text{m}$, oil volume fraction $\phi = 10\%$, and surfactant micelle volume fractions (a) $\phi_m = 0$ and (b) $\phi_m = 9.2 \times 10^{-3}$.

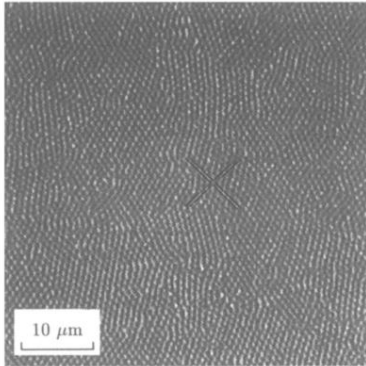


FIG. 3. A picture showing, on a polycrystalline sample, the long-range ordering of the dense phase. The droplet diameter is $\sigma=0.93 \mu\text{m}$.